Published in final edited form as:
Cancer Prev Res (Phila). 2011 January ; 4(1): 51–64. doi:10.1158/1940-6207.CAPR-10-0180.

Interleukin 6 But Not T Helper 2 Cytokines Promotes Lung Carcinogenesis

Cesar Ochoa Perez[1,2,*], **Seyedeh Golsar Mirabolfathinejad**[1,*], **Ana Ruiz Venado**[2], **Scott E. Evans**[1,3], **Mihai Gagea**[4], **Christopher M. Evans**[1,3], **Burton F. Dickey**[1,3], and **Seyed Javad Moghaddam**[1]

[1]Departments of Pulmonary Medicine, The University of Texas M. D. Anderson Cancer Center, Houston, Texas, USA

[2]Tecnológico de Monterrey School of Medicine, Monterrey, Nuevo León, Mexico

[3]Institute of Biosciences and Technology, Center for Inflammation and Infection, Houston, Texas, USA

[4]Department of Veterinary Medicine & Surgery, The University of Texas M. D. Anderson Cancer Center, Houston, Texas, USA

Abstract

Several epidemiologic studies have found that smokers with chronic obstructive pulmonary disease (COPD), an inflammatory disease of the lung, have an increased risk of lung cancer compared to smokers without COPD. We have shown a causal role for COPD-like airway inflammation in lung cancer promotion in the $CCSP^{Cre}$/LSL–K-ras^{G12D} mouse model (CC-LR). In contrast, existing epidemiologic data do not suggest any definite association between allergic airway inflammation and lung cancer. To test this, CC-LR mice were sensitized to ovalbumin (OVA) then challenged with an OVA aerosol weekly for eight weeks. This resulted in eosinophilic lung inflammation associated with increased levels of T helper 2 cytokines and mucous metaplasia of airway epithelium, similar to what is seen in asthma patients. However, this type of inflammation did not result in a significant difference in lung surface tumor number (49 ± 9 in OVA vs 52 ± 5 in control), in contrast to a 3.2-fold increase with COPD-like inflammation. Gene expression analysis of NTHi-treated lungs showed up-regulation of a different profile of inflammatory genes, including interleukin 6 (IL-6), compared to OVA-treated lungs. Therefore, to determine the causal role of cytokines that mediate COPD-like inflammation in lung carcinogenesis, we genetically ablated IL-6 in CC-LR mice. This not only inhibited intrinsic lung cancer development (1.7-fold), but also inhibited the promoting effect of extrinsic COPD-like airway inflammation (2.6-fold). We conclude that there is a clear specificity for the nature of inflammation in lung cancer promotion, and IL-6 has an essential role in lung cancer promotion.

Keywords

lung cancer; inflammation; COPD; asthma; IL-6

Corresponding Author: Seyed Javad Moghaddam, M.D., Department of Pulmonary Medicine, The University of Texas M. D. Anderson Cancer Center, 1515 Holcombe Boulevard, Unit 1100, Houston, TX 77030, Tel: 713-563-0423, Fax: 713-563-0411, smoghadd@mdanderson.org.
*These authors contributed equally to the manuscript.

Introduction

Worldwide, lung cancer is the leading cause of cancer mortality, and is expected to account for 30% of all male and 26% of all female cancer deaths in 2009 (1). Cigarette smoking is the principal cause of lung carcinogenesis, and is thought to do so primarily by inducing DNA mutations (2). However, several studies have found that smokers with chronic obstructive pulmonary disease (COPD), an inflammatory disease of the airways and alveoli, have an increased risk of lung cancer (1.3–4.9-fold) compared to smokers with comparable cigarette exposure but without COPD (3-5). It has also been shown that increased lung cancer mortality is associated with a history of COPD, even among persons who had never been active smokers (6). These facts suggest a link between airway inflammation and lung cancer.

We have previously established a COPD-like mouse model of airway inflammation induced by repetitive exposure to an aerosolized lysate of non-typeable *Haemophilus influenzae* (NTHi) (7), which is the most common bacterial colonizer of airways in COPD patients (8,9). We have shown that this type of inflammation enhances lung carcinogenesis in a K-ras induced mouse model (10). The predominant inflammatory cell types in subjects with COPD are neutrophils, macrophages, CD8+ T lymphocytes, and T helper (Th) 1 and Th17 CD4+ lymphocytes (11,12). The most prominent cytokines are TNF, IL-6, IFN-γ, and IL-8 (11,12), and this profile of inflammatory cells and cytokines is recapitulated in our mouse model of COPD-like airway inflammation (7). This is in contrast to asthma, in which the predominant inflammatory cell types are eosinophils, mast cells and Th2-type CD4+ lymphocytes, and the key cytokines are the Th2 cytokines IL-4, IL-5, IL-9, and IL-13, in both animal models and patients (13-16). Of interest, existing epidemiologic data do not suggest an association between allergic inflammation of the airways and lung cancer, and some even suggest a protective role (17-21). In the current study we tested the role of allergic airway inflammation in lung carcinogenesis in mice and found that it neither promotes nor protects against lung cancer in a K-ras mutant mouse model (CC-LR mouse).

IL-6 is the most highly elevated cytokine in our mouse model of COPD-like inflammation (7), and has been implicated in inflammatory responses in human COPD (11,12). The overexpression of IL-6 in the airways in murine models results in emphysema-like airspace enlargement and airway inflammation (22). IL-6 is also involved in human cancers (23) and is a critical tumor promoter in animal models (24-28). Therefore, to dissect the mechanism of lung cancer promotion by COPD-like inflammation, we tested the role of IL-6, and demonstrated an essential role for this inflammatory cytokine.

Materials and Methods

Animals

Specific pathogen–free, 5 to 6 week old wild type (WT) female C57BL/6 mice were purchased from Harlan (Indianapolis, IN). $CCSP^{Cre}$/LSL–K-ras^{G12D} mice (CC-LR) were generated as previously described (10). Briefly, this is a mouse generated by crossing a mouse harboring the LSL–K-ras^{G12D} allele with a mouse containing Cre recombinase inserted into the Clara cell secretory protein (CCSP) locus (10). CC-LR/IL6KO mice were generated by crossing CC-LR mice to a previously generated mouse with a targeted mutation in exon 2 of the IL-6 gene (IL-6 KO mouse) (29). IL-6 KO mice were purchased from the Jackson Laboratory (Bar Harbor, ME). All mice were housed in specific pathogen–free conditions, and handled in accordance with the Institutional Animal Care and Use Committee of M. D. Anderson Cancer Center. Mice were monitored daily for evidence of disease or death.

Ovalbumin Sensitization and Aerosol Exposure

CC-LR and WT mice were sensitized to ovalbumin (OVA) administered by intraperitoneal (IP) injection weekly for two weeks at age of 6 weeks (20 μg ovalbumin Grade V, 2.25 mg alum in saline, pH7.4; Sigma, St. Louis, MO). Starting at the age of 8 weeks, sensitized mice were exposed for 30 minutes to an aerosol of 2.5% ovalbumin in 0.9% saline supplemented with 0.02% antifoam A silicon polymer (Sigma) via an AeroMist CA-209 compressed gas nebulizer (CIS-US, Bedford, MA) in the presence of room air supplemented with 5% CO2 (30). Mice were challenged weekly with aerosols for eight weeks.

NTHi Lysate Aerosol Exposure

A lysate of NTHi strain 12 was prepared as previously described (7), the protein concentration was adjusted to 2.5 mg/ml in phosphate buffered saline (PBS), and the lysate was frozen in 10 ml aliquots at -80°C. To deliver the lysate to mice by aerosol, a thawed aliquot was placed in an AeroMist CA-209 nebulizer (CIS-US) driven by 10 l/min of room air supplemented with 5% CO2 for 20 min. CC-LR and CC-LR/IL6KO mice were exposed to the lysate starting at 6 weeks of age once a week for 8 weeks.

Assessment of Lung Tumor Burden and Inflammation

On the first day after the final NTHi or OVA exposure, animals were euthanized by IP injection of a lethal dose of avertin (Sigma). In all mice (n=8 per group per time point), lung surface tumor numbers were counted, then in some of them (n=4 per group per time point) the lungs were prepared for histological analysis as described below. In other mice (n=4 per group per time point), bronchoalveolar lavage fluid (BALF) was obtained by sequentially instilling and collecting two aliquots of 1 ml PBS through a tracheostomy cannula. Total leukocyte count was determined using a hemacytometer, and cell populations were determined by cytocentrifugation of 300 μl of BALF followed by Wright-Giemsa staining. The remaining BALF (~1,400 μl) was centrifuged at 1,250 × *g* for 10 min, and supernatants were collected and stored at -70°C. Cytokine concentrations were measured in duplicate by multiplexed sandwich ELISA using SearchLight Proteome Arrays (Aushon Biosystems, Billerica, MA).

Histochemistry

The tracheas of euthanized mice were cannulated with PE-50 tubing and sutured into place. The lungs were infused with 10% buffered formalin (Sigma), removed and placed in 10% buffered formalin for 18 h. Tissues then were transferred to 75% ethanol, embedded in paraffin blocks and sectioned at 5-μm thickness. The sections on glass slides were dried at 60°C for 15 min, and then were deparaffinized and stained with hematoxylin and eosin (H&E) by incubating the tissues in Harris hematoxylin (Sigma) followed by serial eosin (Sigma) and graded ethanol steps. The H&E stained slides were examined by a pathologist blinded to genotype and treatment, and the proliferative lesions of the lungs were evaluated in accordance with the recommendations of the Mouse Models of Human Cancer Consortium (31). The severity of inflammatory lesions of the lungs were scored from 1 to 4 as follows: grade 1 – minimal, lesions affect less than 10% of tissue; grade 2 – mild, lesions affect 10-20% of tissue; grade 3 – moderate, lesions affect 21-40% of tissue; and grade 4 – marked or severe, lesions affect 41-100% of the tissue.

For fluorescent labeling of mucin, tissues were stained using a periodic acid fluorescent Schiff (PAFS) staining procedure in which acriflavine was substituted for pararosaniline as described previously (30). Briefly, tissues were oxidized in 1% periodic acid (10 min), rinsed, treated with acriflavine fluorescent Schiff's reagent (0.5% acriflavine HCl, 1% sodium metabisulfite, 0.01 N HCl) for 20 min, rinsed in double deionized H_2O, and rinsed 2

× 5 minutes in acid alcohol (0.1 N HCl in 70% ethanol). Slides were dehydrated in graded ethanol solutions and allowed to air dry in the dark. Once dry, PAFS-stained slides were coverslipped with Canada balsam mounting medium (50% Canada balsam resin, 50% methyl salicylate; Fisher Chemicals), then analyzed with fluorescence microscopy as previously described, with mucin granules showing red fluorescence and nuclei and cytoplasm showing green fluorescence (30).

Gene Expression Analysis

Mice treated with the aerosolized NTHi lysate or OVA aerosol were euthanized on day one after the last exposure for comparison (n=4 per group). To reduce the lung leukocyte burden, the pulmonary vasculature was perfused and the airways lavaged with PBS. The lungs were mechanically homogenized, then total RNA was isolated from lung homogenates using the RNeasy system (Qiagen, Valencia, CA), and cRNA was synthesized and amplified from equal masses of total RNA using the Ilumina TotalPrep RNA amplification kit (Ambion, Austin, TX). Amplified cRNA was hybridized and labeled on Sentrix Mouse-8 Expression BeadChips (Illumina, San Diego, CA), then scanned on a BeadStation 500 (Illumina). Primary microarray data were deposited at the NCBI Gene Expression Omnibus (http://www.ncbi.nlm.nih.gov/geo/) consistent with minimum information about a microarray experiment (MIAME) standards (GEO Accession GSE19605). Primary signal intensity was background-subtracted and normalized to untreated groups (wild type or K-ras mutants) using a rank-invariant algorithm. Differentially expressed genes were identified using Illumina BeadStudio software. Genes with differential scores of ≥20 or ≤-20 were considered significantly up- or down-regulated, respectively. Differential score represents the difference in expression of individual genes or cluster genes that are expressed or coexpressed over various conditions, using the Illumina algorithm that incorporates fold-change, detection p-value, and signal intensity standard deviation between replicate beads of each array and signal intensity standard deviation between different arrays in the same treatment group (32,33).

Quantitative RT- PCR (Q-PCR) Analysis

Total RNA was isolated from whole lung according to the TRIzol reagent protocol (Invitrogen, Carlsbad, CA). The cDNA was generated from RNA samples and quantitative RT-PCR using predesigned assays (ABI Systems, Foster City, CA) was performed to assay the expression of the 10 selected up-regulated genes from microarray data. β-actin RNA was measured for reference. PCR was carried out according to a standard protocol (ABI Systems), and products measured on an ABI Prism 7000 sequence detector. Relative expression of each gene was calculated and graphed for comparison among the treatment groups.

Statistical methods

Summary statistics for cell counts in BALF were computed within treatment groups, and analysis of variance with adjustment for multiple comparisons was performed to examine the differences between the mean cell counts of the control group and each of the OVA or NTHi treatment groups. For tumor counts, comparisons of groups were made using Student's t test. Differences were considered significant for $P < 0.05$.

Results

Ovalbumin-induced airway inflammation

In order to test the role of allergic airway inflammation in promotion of lung carcinogenesis, we exposed sensitized WT, CC-LR, and LSL–K-ras^{G12D} littermate control mice to

aerosolized OVA once weekly for 8 weeks. In WT mice, this exposure resulted in more than a 10-fold rise in total leukocyte number one day after the last exposure (not shown). This rise was due to a combination of neutrophils, lymphocytes, macrophages, and eosinophils (Fig 1A). The increase in neutrophil numbers began to decline over the ensuing 2-3 days, followed by a more gradual increase in eosinophils, lymphocytes and macrophages (not shown). This is in contrast to BALF cell populations in NTHi-induced airway inflammation, which are characterized by a very large increase in neutrophil numbers, and no increase in eosinophil numbers (7,10). Analysis of the BALF from LSL–K-ras^{G12D} littermate control mice exposed to aerosolized OVA showed a similar pattern to WT mice (not shown). However, CC-LR mice showed elevated total cell and macrophage numbers even in the absence of exposure to OVA (Fig 1A), as previously described by us and others in models that induce expression of activated K-ras in the airways (10,34,35). Paradoxically, the rise in eosinophil and neutrophil numbers in CC-LR mice after exposure to the OVA aerosol was less than in WT mice (Fig. 1A). This is reminiscent of the declining neutrophil numbers with repetitive exposure of WT mice to the NTHi lysate, and it suggests the development of immune tolerance (7).

Leukocyte recruitment in response to OVA was accompanied by a significant increase in BALF levels of Th2 cytokines (IL-4 and IL-13) and the eosinophil chemokine eotaxin, with mildly increased levels of inflammatory cytokines (IL-6 and TNF) and the neutrophil chemokine KC (Table 1). There was no change in levels of Th1 and Th17 cytokines after repetitive OVA exposure (Table 1), in contrast to NTHi-induced COPD-like airway inflammation where high levels of inflammatory cytokines (IL-6, TNF), TGF-β, IL-17, and KC were detected (data not shown) (7,10). CC-LR mice showed elevated levels of inflammatory cytokines (IL-6; 61.5-fold, TNF; 6.5-fold), IFN-γ; 4.2-fold, IL-17; 9.2-fold, and KC; 6.5-fold even in the absence of OVA exposure compared to WT mice (Table 1).

Histopathologically, both WT and CC-LR mice showed significant airway epithelial mucous metaplasia (red fluorescence) after repetitive aerosol exposure to OVA detected by PAFS staining of lung sections collected two days after the last exposure (Fig. 1B), indicating effective function of OVA-induced inflammation in producing an asthmatic airway epithelial phenotype. There were numerous mixed inflammatory cells infiltrated around the airways and blood vessels in the lungs of 12- and 16-week old control and CC-LR mice after 4 and 8 weekly OVA aerosol exposures (Fig. 2A). In addition, mild to moderate numbers of macrophages were infiltrated diffusely in the alveoli of these mice. Of note, in contrast to increased infiltration of lung parenchyma with macrophages after chronic OVA exposure, less macrophages were seen in BALF of CC-LR mice exposed to OVA (Fig. 1A). This is not uncommon because BALF only provides information about the cells within the alveolar air spaces that readily detach from the septae. Cells infiltrating the lung parenchyma and tumors are not likely to be present in BALF as previously described (36).

Effect of ovalbumin-induced airway inflammation on lung tumor progression

Histological examination revealed that the lungs of 16-week old CC-LR mice not exposed to OVA contained an average of 33 foci of bronchiolar and/or alveolar hyperplasia, 8 foci of atypical adenomatous hyperplasia and 0.7 alveolar adenomas (Fig. 2A). These lesions were associated with minimal infiltration (grade 1) of macrophages and occasional lymphocytes in the alveolar parenchyma and perivascular area. Unlike the mice unexposed to OVA, the 12- and 16-week-old CC-LR mice exposed weekly to the OVA aerosol had more numerous macrophages, neutrophils and lymphocytes infiltrated around the airways and blood vessels (grade 2 and 3) and diffusely into the alveolar parenchyma (grade 2) (Fig. 2A). Although the numbers of infiltrated inflammatory cells were significantly increased in CC-LR mice exposed to OVA in comparison with CC-LR mice not exposed to OVA, the CC-LR mice exposed to OVA had fewer proliferative lung lesions. The CC-LR mice exposed to OVA

had an average of 22 foci of hyperplasia, 4 foci of atypical adenomatous hyperplasia and no adenomas or adenocarcinomas. Additionally, the proliferative lesions were less extensive, affecting a slightly lower percent of the pulmonary parenchyma in CC-LR mice exposed to OVA (Fig. 2A). Most hyperplastic lesions of these lungs consisted of a combination of papillary hyperplasia of bronchiolar epithelium and alveolar hyperplasia. Only a few hyperplastic lung lesions affected either the bronchioles or the alveoli alone. Atypical adenomatous hyperplasia affected the terminal bronchioles and alveoli and had a higher degree of hyperplasia associated with cellular atypia, significant anisocytosis and anisokaryosis, hyperchromasia, and dysplastic growth of epithelial cells, but without formation of a distinct solid mass as in adenoma or carcinoma. Adenomas were well-circumscribed areas of cuboidal or columnar cells lining the alveoli and replacing completely the alveolar spaces, making solid masses less than 5 mm in diameter. Adenomatous lesions larger than 5 mm in diameter, or smaller solid lesions that had marked cytological atypia, numerous mitoses, and evidence of invasion of the surrounding tissues or vasculature were classified as pulmonary adenocarcinomas.

The effect of airway inflammation induced by the OVA aerosol on lung tumor progression was analyzed quantitatively by determining the number of tumors visible macroscopically on the pleural surface of the lungs in CC-LR mice. As shown in Figure 2B, in contrast to NTHi-induced airway inflammation which promotes tumor development 3.2-fold (gray line) (10), OVA did not change the number of lung surface tumors in CC-LR mice after 4 (22 ± 3 in OVA-exposed vs 26 ± 6 in control mice) or 8 weekly exposures (49 ± 9 in OVA-exposed vs 52 ± 5 in control mice, black lines). No tumors were observed macroscopically on the lung surface of control WT and LSL–K-ras^{G12D} mice exposed to the OVA aerosol for a similar duration (data not shown).

Effect of NTHi- and OVA-induced airway inflammation on gene expression in the lung

To gain insight into the mechanism of cancer promotion by intrinsic Ras-induced inflammation and by extrinsic NTHi-induced COPD-like inflammation, but not by OVA-induced asthma-like airway inflammation, we compared the gene expression profiles of NTHi-treated and OVA-treated lungs one day after the last exposure. Requiring a differential score of ≥20 to define up-regulated genes and ≤-20 to define down-regulated genes, we identified 149 differentially expressed genes (DEGs) in untreated CC-LR mice (22 decreased, 127 increased) compared to untreated WT mice. We also identified 253 DEGs in NTHi-treated WT mice (16 decreased, 253 increased) compared to non-treated WT mice, and 485 DEGs in NTHi-treated CC-LR mice (16 decreased, 485 increased) compared to non-treated CC-LR mice. Conversely, chronic OVA exposure resulted in a much less pronounced differential gene expression pattern, with only 3 DEGs in chronically OVA-exposed WT mice and no DEGs in chronically OVA-exposed CC-LR mice, compared to untreated mice. The differentially expressed genes encode a broad array of proteins involved in inflammation and immune responses, including cytokines and chemokines, pattern recognition receptors, intracellular signaling proteins, and numerous proteins involved in tumor development, including ones responsible for cell cycle and growth, cell death and apoptosis, angiogenesis, invasion, and metastasis (Fig. 3A, and Table 2).

In order to validate the microarray data, we measured transcripts of some up-regulated genes involved in inflammation and tumor promotion in the lungs of WT, CC-LR, and CC-LR exposed to NTHi or OVA mice by Q-PCR (Fig. 3B). The results were in agreement with microarray data showing upregulation of these genes in response to NTHi.

Effect of IL-6 deletion on lung cancer promotion

In gene expression analysis of whole lung, CC-LR mice showed high expression of the IL-6 gene (14-fold) compared to WT mice (Table 2). Similarly, IL-6 protein levels were higher in BALF of CC-LR mice (61-fold) even in the absence of COPD-like airway inflammation (Table 1 and ref 10). Repetitive NTHi exposure further increased expression of the IL-6 gene (1.6-fold) in CC-LR mice (Table 1), whereas repetitive OVA exposure actually decreased IL-6 expression (3.9-fold, Table 1). This is consistent with our previous results that IL-6 protein levels were greatly increased in BALF after NTHi exposure (10). These findings prompted us to investigate the role of IL-6 in K-ras induced intrinsic inflammation and cancer promotion by extrinsic COPD-like airway inflammation by crossing CC-LR mice with IL-6 KO mice, then exposing CC-LR and CC-LR/IL6KO mice to the aerosolized NTHi lysate once weekly for 8 weeks from age 6 weeks. Surprisingly, lack of IL-6 did not change the BALF inflammatory cell profile of CC-LR mice at baseline or after inducing COPD-like inflammation (Fig. 4A). However lack of IL-6 resulted in a 41% reduction in the number of grossly visible tumors on the lung surface compared to age and sex matched control CC-LR mice (26 ± 7 in CC-LR/IL6KO vs. 44 ± 6 in CC-LR) (Fig. 4B). In CC-LR mice exposed to weekly NTHi aerosol, IL-6 deficiency reduced the number of visible surface tumors by 62% (60 ± 2 in CC-LR/IL6KO NTHi treated vs. 156 ± 9 in CC-LR NTHi treated) (Fig. 4B). Histopathologic analysis showed that the lungs from CC-LR/IL6KO mice had fewer and less extensive lesions of hyperplasia, atypical adenomatous hyperplasia, and neoplasia, and a lower percentage of the total pulmonary parenchyma was affected in comparison with CC-LR mice in the presence and absence of NTHi-induced airway inflammation (Fig. 4C). The non-NTHi-treated CC-LR/IL6KO mice (lower left panel) had less numerous lesions of atypical adenomatous hyperplasia and neoplasia than non-NTHi-treated CC-LR mice (upper left panel). The NTHi treatment caused similarly severe inflammation (grade 4) in the lungs of CC-LR and CC-LR/IL6KO mice, but the lesions of bronchiolar and alveolar hyperplasia, atypical adenomatous hyperplasia, and neoplasia were less extensive and less numerous in NTHi-treated CC-LR/IL6KO mice (right lower panel) compared to the NTHi-treated CC-LR mice (right upper panel).

Discussion

The likelihood of developing lung cancer within 10 years is 3-fold greater in patients with mild to moderate COPD and 10-fold greater in patients with severe COPD compared to smokers with normal lung function (37). COPD is thought to be caused by the lung parenchymal response to inflammation from cigarette smoke and from bacterial colonization of smoke-injured airways (8,38). We previously showed the role of COPD-like inflammation in promotion of lung carcinogenesis in a K-ras induced mouse model of lung cancer (10). In contrast, there is no definite epidemiologic association between allergic type airway inflammation and lung cancer, with most studies leaning toward a protective or neutral role for this type of inflammation in cancer promotion (17-21). In the current study we have shown the neutral role of asthma-like (Th2 mediated) airway inflammation in lung cancer promotion in mice.

Traditionally, Th1 cells are considered to facilitate tissue destruction and tumor rejection by providing help to cytotoxic CD8+ T cells, while Th2 cells are considered to induce antibody production by B cells and polarize immunity away from an anti-tumor response (39). Consistent with this, allergen-induced pulmonary inflammation resulted in a more than 3-fold increase in lung metastases of intravenously injected melanoma cells in mice (40). This was dependent on CD4+ T-cell activities but independent of the induced eosinophilia. Recently, an indirect role for IL-4-expressing CD4+ T lymphocytes (Th2 cells) in invasion and subsequent metastasis of mammary adenocarcinomas has been reported (41). Th2 cells enhanced metastasis by directly enhancing tumor-promoting properties of tumor-associated

macrophages (TAMs) and subsequent activation of epidermal growth factor receptor signaling in malignant mammary epithelial cells. Furthermore in a different study, lack of IL-4Rα resulted in smaller tumor size but no change in tumor multiplicity after urethane injection due to inhibition of the tumor-promoting phenotype of TAMs (36). Whereas these studies showed an indirect role for Th2 cells in promoting lung metastasis and of IL-4 in the size of metastases, there is no evidence of a direct promoting role for this type of immune response on primary cancer in any organ, including the lung, of which we are aware.

Using microarray analysis of the lungs from WT and CC-LR mice and its validation by Q-PCR, we identified many genes with increased transcript levels after chronic NTHi exposure but not after chronic OVA exposure. The majority of upregulated genes in the lungs of NTHi-exposed mice were genes involved in inflammation and immune responses (Fig. 3 and Table 2). The remainder includes genes involved in cell growth, proliferation, invasion, angiogenesis, and metastasis. Therefore we propose that NTHi, but not OVA, causes a specific inflammatory and innate immune response in the lungs of tumor-bearing mice by up-regulating genes involved in recruitment of inflammatory cells including neutrophils, macrophages, and adaptive immune cells (probably Th17 cells), and activating immune regulatory pathways (NF-κB and STAT3 pathways) in lung epithelial cells that results in proliferation, angiogenesis, invasion and metastasis (see below).

Among the upregulated inflammatory genes, IL-6 showed a very high expression level in BALF (7,10) and lung tissue (Table 2) after NTHi exposure in WT and CC-LR mice, whereas it decreased after OVA exposure (Table 1). BALF of CC-LR mice showed a high level of IL-6 even without NTHi exposure which actually was suppressed by OVA exposure (Table 1). The IL-6 pathway has been found to be one of the mechanisms linking inflammation to cancer (42). Ras activation induces the secretion of IL-6 in different cell types, and knockdown of IL-6, genetic ablation of the IL-6 gene, or treatment with a neutralizing IL-6 antibody all retard Ras-driven tumorigenesis *in vitro* (25). IL-6 appears to act in a paracrine fashion to promote angiogenesis and tumor growth. It has also been found that IL-6 is a critical tumor promoter during early colitis-associated cancer (27). It is produced by lamina propria myeloid cells and protects normal and premalignant intestinal epithelial cells from apoptosis. We show here an essential role for IL-6 in Ras-induced lung cancer development and its promotion by extrinsic COPD-like inflammation using genetic deletion of IL-6 in CC-LR mice (Fig. 4).

The proliferative and survival effects of IL-6 on epithelial cells are mediated by STAT3 (27). Persistently activated STAT3 increases tumor cell proliferation, survival, angiogenesis and invasion (23,43). Overexpression of STAT3 in alveolar type II epithelial cells of mice leads to severe pulmonary inflammation and spontaneous bronchoalveolar adenocarcinoma (44). Activated STAT3 also mediates tumor-promoting inflammation by activating pro-oncogenic inflammatory pathways including NF-κB (43,45). NF-κB is constitutively active in COPD patients (46), smokers (47), and in lung tumors (48), where it upregulates antiapoptotic and other oncogenic genes (49). Overexpression of the RelA subunit of the NF-kB complex in the lung yields increased alveolar type I and type II cells through decreased apoptosis of epithelial cells (50). It has been also shown that tobacco smoke promotes lung tumorigenesis by triggering IKKβ-dependent inflammation (51), and NF-κB inhibition in the lungs suppresses airway inflammation (52-55) and urethane-induced lung cancer (56).

Maintenance of NF-κB activity in tumors requires STAT3. STAT3-mediated maintenance of NF-κB activity occurs in both cancer cells and tumor-associated hematopoietic cells (57). We have also found significant activation of STAT3 and NF-κB pathways in the CC-LR model after inducing COPD-like inflammation (Fig. 3A,Table 2). IL-13 contributes to

asthma by activating epithelial-cell STAT6 (58). Among Th2 cytokines, IL-13 seems to be both necessary and sufficient, because blockade of IL-13 markedly inhibits allergen-induced airway hyperresponsiveness (AHR), mucus production and eosinophilia (59,60), and IL-13 delivery to the lung or transgenic IL-13 overexpression in the airway epithelium causes all of these effects (59-61). Mice lacking STAT6 are protected from all pulmonary effects of IL-13, and reconstitution of STAT6 only in epithelial cells is sufficient for IL-13-induced AHR and mucus production (58). These data further explain the differential effects of asthma-type airway inflammation on lung cancer promotion compared to COPD-like airway inflammation.

In addition to their role in extracellular matrix turnover and cancer cell migration, MMPs regulate the tumor microenvironment through signaling pathways that control cell growth, inflammation, or angiogenesis (62). They modulate the function of cytokines and chemokines which can promote cancer cell survival in an NF-κB-dependent manner. Among MMPs, MMP12 plays a critical role in smoking-induced COPD (63), and its expression correlates with early cancer-related deaths in NSCLC (64). Furthermore, overexpression of MMP-12 in lung epithelial cells led to inflammatory cell infiltration, increased epithelial growth, spontaneous emphysema and bronchioalveolar adenocarcinoma (65). This was associated with increased level of IL-6 in BALF, which activated STAT3 in alveolar type II epithelial cells and increased expression of its downstream genes in the lung. We have also found up-regulation of MMPs, especially MMP-12, in lung tissue with NTHi-induced COPD-like inflammation (Fig. 3B, and Table 2), further confirming a role for the IL-6/STAT3 pathway through MMPs in promotion of lung cancer by COPD-like inflammation.

New evidence also points at the IL-6/STAT3 pathway as one of the pathways coordinating the interface between adaptive and innate immunity (42), probably by inducing a pro-tumor Th17 response (66) and opposing STAT1 mediated Th1 anti-tumor immune responses (43,45). Th17 cells produce IL-17, and IL-17 induces more production of IL-6 by epithelial cells and fibroblasts, which in turn activates STAT3, up-regulating prosurvival and proangiogenic genes (66-68). We have also found increased numbers of Th17 cells and elevated IL-17 levels in response to NTHi in the lung (data not shown), indicating a skewed adaptive immune response toward a pro-tumor Th17 response (manuscript in preparation).

In conclusion we propose that exposure of the airway to smoke particulates and microbial products contribute to COPD-like lung inflammation and lung cancer promotion. This is mediated by release of IL-6 and other inflammatory cytokines such as TNF from epithelial and innate immune cells secondary to NF-kB activation, which in turn further activates the STAT3 and NF-κB pathways in airway epithelium. STAT3 and NF-κB cooperate to activate pro-survival, anti-apoptotic, and pro-angiogenic signals that are accompanied by skewing towards a pro-tumoral adaptive immune response (Th17 response). Full elucidation of this model will provide the basis for testing of the efficacy of rationally directed anti-inflammatory therapies in preventing carcinogenesis in patients at high risk for tumor development on the basis of inflammation related to COPD.

Acknowledgments

We thank Derek Larson, Angelito P. De Villa, and Blaga Iankova for their technical assistance in the completion of this project.

This work was supported by grant [UO1 CA105352] from the National Cancer Institute, and [LCD-114696-N] from the American Lung Association/LUNGevity Foundation.

References

1. Jemal A, Siegel R, Ward E, et al. Cancer statistics, 2009. CA Cancer J Clin. 2009; 59:225–49. [PubMed: 19474385]
2. Stellman SD, Takezaki T, Wang L, et al. Smoking and lung cancer risk in American and Japanese men: an international case-control study. Cancer Epidemiol Biomarkers Prev. 2001; 10:1193–99. [PubMed: 11700268]
3. Shacter E, Weitzman SA. Chronic inflammation and cancer. Oncology (Williston Park). 2002; 16:217–26. 229. [PubMed: 11866137]
4. Tockman MS, Anthonisen NR, Wright EC, Donithan MG. Airways obstruction and the risk for lung cancer. Ann Intern Med. 1987; 106:512–18. [PubMed: 3826952]
5. Skillrud DM, Offord KP, Miller RD. Higher risk of lung cancer in chronic obstructive pulmonary disease. A prospective, matched, controlled study. Ann Intern Med. 1986; 105:503–07. [PubMed: 3752756]
6. Turner MC, Chen Y, Krewski D, Calle EE, Thun MJ. Chronic obstructive pulmonary disease is associated with lung cancer mortality in a prospective study of never smokers. Am J Respir Crit Care Med. 2007; 176:285–90. [PubMed: 17478615]
7. Moghaddam SJ, Clement CG, De la Garza MM, et al. Haemophilus influenzae lysate induces aspects of the chronic obstructive pulmonary disease phenotype. Am J Respir Cell Mol Biol. 2008; 38:629–38. [PubMed: 18096867]
8. King PT, Hutchinson PE, Johnson PD, et al. Adaptive immunity to nontypeable Haemophilus influenzae. Am J Respir Crit Care Med. 2003; 167:587–92. [PubMed: 12433671]
9. Murphy TF. Haemophilus influenzae in chronic bronchitis. Semin Respir Infect. 2000; 15:41–51. [PubMed: 10749549]
10. Moghaddam SJ, Li H, Cho SN, et al. Promotion of lung carcinogenesis by chronic obstructive pulmonary disease-like airway inflammation in a K-ras-induced mouse model. Am J Respir Cell Mol Biol. 2009; 40:443–53. [PubMed: 18927348]
11. Saetta M, Di Stefano A, Turato G, et al. CD8+ T-lymphocytes in peripheral airways of smokers with chronic obstructive pulmonary disease. Am J Respir Crit Care Med. 1998; 157:822–26. [PubMed: 9517597]
12. Barnes PJ. Chronic obstructive pulmonary disease. N Engl J Med. 2000; 343:269–80. [PubMed: 10911010]
13. Murdoch JR, Lloyd CM. Chronic inflammation and asthma. Mutat Res. 2009
14. Van Hove CL, Maes T, Joos GF, Tournoy KG. Chronic inflammation in asthma: a contest of persistence vs resolution. Allergy. 2008; 63:1095–109. [PubMed: 18616676]
15. Zosky GR, Sly PD. Animal models of asthma. Clin Exp Allergy. 2007; 37:973–88. [PubMed: 17581191]
16. Kumar RK, Foster PS. Modeling allergic asthma in mice: pitfalls and opportunities. Am J Respir Cell Mol Biol. 2002; 27:267–72. [PubMed: 12204888]
17. Merrill RM, Isakson RT, Beck RE. The association between allergies and cancer: what is currently known? Ann Allergy Asthma Immunol. 2007; 99:102–16. [PubMed: 17718097]
18. Ramanakumar AV, Parent ME, Menzies D, Siemiatycki J. Risk of lung cancer following nonmalignant respiratory conditions: evidence from two case-control studies in Montreal, Canada. Lung Cancer. 2006; 53:5–12. [PubMed: 16733074]
19. Gorlova OY, Zhang Y, Schabath MB, et al. Never smokers and lung cancer risk: a case-control study of epidemiological factors. Int J Cancer. 2006; 118:1798–804. [PubMed: 16217766]
20. Turner MC, Chen Y, Krewski D, Ghadirian P. An overview of the association between allergy and cancer. Int J Cancer. 2006; 118:3124–32. [PubMed: 16395696]
21. Littman AJ, Thornquist MD, White E, et al. Prior lung disease and risk of lung cancer in a large prospective study. Cancer Causes Control. 2004; 15:819–27. [PubMed: 15456995]
22. Kuhn C III, Homer RJ, Zhu Z, et al. Airway hyperresponsiveness and airway obstruction in transgenic mice. Morphologic correlates in mice overexpressing interleukin (IL)-11 and IL-6 in the lung. Am J Respir Cell Mol Biol. 2000; 22:289–95. [PubMed: 10696065]

23. Hodge DR, Hurt EM, Farrar WL. The role of IL-6 and STAT3 in inflammation and cancer. Eur J Cancer. 2005; 41:2502–12. [PubMed: 16199153]
24. Naugler WE, Sakurai T, Kim S, et al. Gender disparity in liver cancer due to sex differences in MyD88-dependent IL-6 production. Science. 2007; 317:121–24. [PubMed: 17615358]
25. Ancrile B, Lim KH, Counter CM. Oncogenic Ras-induced secretion of IL6 is required for tumorigenesis. Genes Dev. 2007; 21:1714–19. [PubMed: 17639077]
26. Maeda S, Hikiba Y, Sakamoto K, et al. Ikappa B kinasebeta/nuclear factor-kappaB activation controls the development of liver metastasis by way of interleukin-6 expression. Hepatology. 2009; 50:1851–60. [PubMed: 19821485]
27. Grivennikov S, Karin E, Terzic J, et al. IL-6 and Stat3 are required for survival of intestinal epithelial cells and development of colitis-associated cancer. Cancer Cell. 2009; 15:103–13. [PubMed: 19185845]
28. Grivennikov S, Karin M. Autocrine IL-6 signaling: a key event in tumorigenesis? Cancer Cell. 2008; 13:7–9. [PubMed: 18167335]
29. Kopf M, Baumann H, Freer G, et al. Impaired immune and acute-phase responses in interleukin-6-deficient mice. Nature. 1994; 368:339–42. [PubMed: 8127368]
30. Evans CM, Williams OW, Tuvim MJ, et al. Mucin is produced by clara cells in the proximal airways of antigen-challenged mice. Am J Respir Cell Mol Biol. 2004; 31:382–94. [PubMed: 15191915]
31. Nikitin AY, Alcaraz A, Anver MR, et al. Classification of proliferative pulmonary lesions of the mouse: recommendations of the mouse models of human cancers consortium. Cancer Res. 2004; 64:2307–16. [PubMed: 15059877]
32. Dunning MJ, Barbosa-Morais NL, Lynch AG, Tavare S, Ritchie ME. Statistical issues in the analysis of Illumina data. BMC Bioinformatics. 2008; 9:85. [PubMed: 18254947]
33. Novak JP, Miller MC III, Bell DA. Variation in fiberoptic bead-based oligonucleotide microarrays: dispersion characteristics among hybridization and biological replicate samples. Biol Direct. 2006; 1:18. [PubMed: 16787528]
34. Ji H, Houghton AM, Mariani TJ, et al. K-ras activation generates an inflammatory response in lung tumors. Oncogene. 2006; 25:2105–12. [PubMed: 16288213]
35. Wislez M, Spencer ML, Izzo JG, et al. Inhibition of mammalian target of rapamycin reverses alveolar epithelial neoplasia induced by oncogenic K-ras. Cancer Res. 2005; 65:3226–35. [PubMed: 15833854]
36. Redente EF, Dwyer-Nield LD, Barrett BS, Riches DW, Malkinson AM. Lung tumor growth is stimulated in IFN-gamma-/- mice and inhibited in IL-4Ralpha-/- mice. Anticancer Res. 2009; 29:5095–101. [PubMed: 20044622]
37. Mannino DM, Aguayo SM, Petty TL, Redd SC. Low lung function and incident lung cancer in the United States: data From the First National Health and Nutrition Examination Survey follow-up. Arch Intern Med. 2003; 163:1475–80. [PubMed: 12824098]
38. Barnes PJ. New concepts in chronic obstructive pulmonary disease. Annu Rev Med. 2003; 54:113–29. [PubMed: 12359824]
39. Ostrand-Rosenberg S, Sinha P. Myeloid-derived suppressor cells: linking inflammation and cancer. J Immunol. 2009; 182:4499–506. [PubMed: 19342621]
40. Taranova AG, Maldonado D III, Vachon CM, et al. Allergic pulmonary inflammation promotes the recruitment of circulating tumor cells to the lung. Cancer Res. 2008; 68:8582–89. [PubMed: 18922934]
41. DeNardo DG, Barreto JB, Andreu P, et al. CD4(+) T cells regulate pulmonary metastasis of mammary carcinomas by enhancing protumor properties of macrophages. Cancer Cell. 2009; 16:91–102. [PubMed: 19647220]
42. Naugler WE, Karin M. The wolf in sheep's clothing: the role of interleukin-6 in immunity, inflammation and cancer. Trends Mol Med. 2008; 14:109–19. [PubMed: 18261959]
43. Yu H, Pardoll D, Jove R. STATs in cancer inflammation and immunity: a leading role for STAT3. Nat Rev Cancer. 2009; 9:798–809. [PubMed: 19851315]

44. Li Y, Du H, Qin Y, et al. Activation of the signal transducers and activators of the transcription 3 pathway in alveolar epithelial cells induces inflammation and adenocarcinomas in mouse lung. Cancer Res. 2007; 67:8494–503. [PubMed: 17875688]
45. Kortylewski M, Yu H. Role of Stat3 in suppressing anti-tumor immunity. Curr Opin Immunol. 2008; 20:228–33. [PubMed: 18479894]
46. Di Stefano A, Caramori G, Oates T, et al. Increased expression of nuclear factor-kappaB in bronchial biopsies from smokers and patients with COPD. Eur Respir J. 2002; 20:556–63. [PubMed: 12358328]
47. Schabath MB, Delclos GL, Martynowicz MM, et al. Opposing effects of emphysema, hay fever, and select genetic variants on lung cancer risk. Am J Epidemiol. 2005; 161:412–22. [PubMed: 15718477]
48. Tang X, Liu D, Shishodia S, et al. Nuclear factor-kappaB (NF-kappaB) is frequently expressed in lung cancer and preneoplastic lesions. Cancer. 2006; 107:2637–46. [PubMed: 17078054]
49. Karin M. Nuclear factor-kappaB in cancer development and progression. Nature. 2006; 441:431–36. [PubMed: 16724054]
50. Londhe VA, Nguyen HT, Jeng JM, et al. NF-kB induces lung maturation during mouse lung morphogenesis. Dev Dyn. 2008; 237:328–38. [PubMed: 18161062]
51. Takahashi H, Ogata H, Nishigaki R, Broide DH, Karin M. Tobacco smoke promotes lung tumorigenesis by triggering IKKbeta- and JNK1-dependent inflammation. Cancer Cell. 2010; 17:89–97. [PubMed: 20129250]
52. Newton R, Holden NS, Catley MC, et al. Repression of inflammatory gene expression in human pulmonary epithelial cells by small-molecule IkappaB kinase inhibitors. J Pharmacol Exp Ther. 2007; 321:734–42. [PubMed: 17322026]
53. Inayama M, Nishioka Y, Azuma M, et al. A novel IkappaB kinase-beta inhibitor ameliorates bleomycin-induced pulmonary fibrosis in mice. Am J Respir Crit Care Med. 2006; 173:1016–22. [PubMed: 16456147]
54. Broide DH, Lawrence T, Doherty T, et al. Allergen-induced peribronchial fibrosis and mucus production mediated by IkappaB kinase beta-dependent genes in airway epithelium. Proc Natl Acad Sci U S A. 2005; 102:17723–28. [PubMed: 16317067]
55. Yang L, Cohn L, Zhang DH, et al. Essential role of nuclear factor kappaB in the induction of eosinophilia in allergic airway inflammation. J Exp Med. 1998; 188:1739–50. [PubMed: 9802985]
56. Stathopoulos GT, Sherrill TP, Cheng DS, et al. Epithelial NF-kappaB activation promotes urethane-induced lung carcinogenesis. Proc Natl Acad Sci U S A. 2007; 104:18514–19. [PubMed: 18000061]
57. Lee H, Herrmann A, Deng JH, et al. Persistently activated Stat3 maintains constitutive NF-kappaB activity in tumors. Cancer Cell. 2009; 15:283–93. [PubMed: 19345327]
58. Kuperman DA, Huang X, Koth LL, et al. Direct effects of interleukin-13 on epithelial cells cause airway hyperreactivity and mucus overproduction in asthma. Nat Med. 2002; 8:885–89. [PubMed: 12091879]
59. Grunig G, Warnock M, Wakil AE, et al. Requirement for IL-13 independently of IL-4 in experimental asthma. Science. 1998; 282:2261–63. [PubMed: 9856950]
60. Wills-Karp M, Luyimbazi J, Xu X, et al. Interleukin-13: central mediator of allergic asthma. Science. 1998; 282:2258–61. [PubMed: 9856949]
61. Zhu Z, Homer RJ, Wang Z, et al. Pulmonary expression of interleukin-13 causes inflammation, mucus hypersecretion, subepithelial fibrosis, physiologic abnormalities, and eotaxin production. J Clin Invest. 1999; 103:779–88. [PubMed: 10079098]
62. Kessenbrock K, Plaks V, Werb Z. Matrix metalloproteinases: regulators of the tumor microenvironment. Cell. 2010; 141:52–67. [PubMed: 20371345]
63. Hautamaki RD, Kobayashi DK, Senior RM, Shapiro SD. Requirement for macrophage elastase for cigarette smoke-induced emphysema in mice. Science. 1997; 277:2002–04. [PubMed: 9302297]
64. Hofmann HS, Hansen G, Richter G, et al. Matrix metalloproteinase-12 expression correlates with local recurrence and metastatic disease in non-small cell lung cancer patients. Clin Cancer Res. 2005; 11:1086–92. [PubMed: 15709175]

65. Qu P, Du H, Wang X, Yan C. Matrix metalloproteinase 12 overexpression in lung epithelial cells plays a key role in emphysema to lung bronchioalveolar adenocarcinoma transition. Cancer Res. 2009; 69:7252–61. [PubMed: 19706765]

66. Wang L, Yi T, Kortylewski M, et al. IL-17 can promote tumor growth through an IL-6-Stat3 signaling pathway. J Exp Med. 2009; 206:1457–64. [PubMed: 19564351]

67. Chen Y, Thai P, Zhao YH, et al. Stimulation of airway mucin gene expression by interleukin (IL)-17 through IL-6 paracrine/autocrine loop. J Biol Chem. 2003; 278:17036–43. [PubMed: 12624114]

68. Molet S, Hamid Q, Davoine F, et al. IL-17 is increased in asthmatic airways and induces human bronchial fibroblasts to produce cytokines. J Allergy Clin Immunol. 2001; 108:430–38. [PubMed: 11544464]

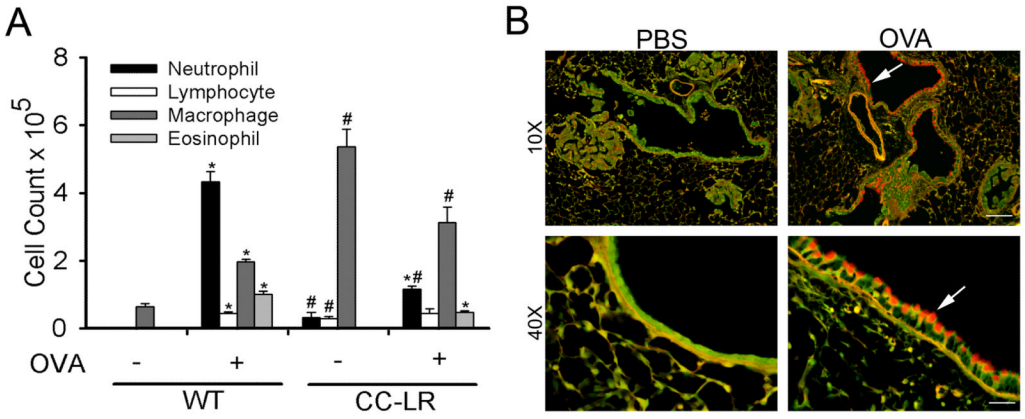

Figure 1. Analysis of lung inflammation after repetitive exposure to the aerosolized ovalbumin (OVA)

WT and CC-LR mice were sensitized by intraperitoneal injection of OVA weekly for two weeks at age 6 weeks. Then starting at age 8 weeks, sensitized mice were exposed to an OVA aerosol weekly for eight weeks. Total and lineage-specific leukocyte numbers in bronchoalveolar lavage fluid (BALF) one day after OVA aerosol exposure are shown (mean ± SE, * = $P < 0.05$ for WT or CC-LR with OVA exposure vs without OVA exposure, # = $P < 0.05$ for WT without OVA exposure vs CC-LR without OVA exposure or WT with OVA exposure vs CC-LR with OVA exposure). (B) PAFS staining for mucin in lungs of CC-LR mice exposed to PBS alone (left two panels), and mice exposed to aerosolized OVA and sacrificed two days after the last exposure (right two panels). Arrows show mucous metaplastic epithelium. Scale bars for 10×, and 40 × panels are 100 μm, and 25 μm respectively.

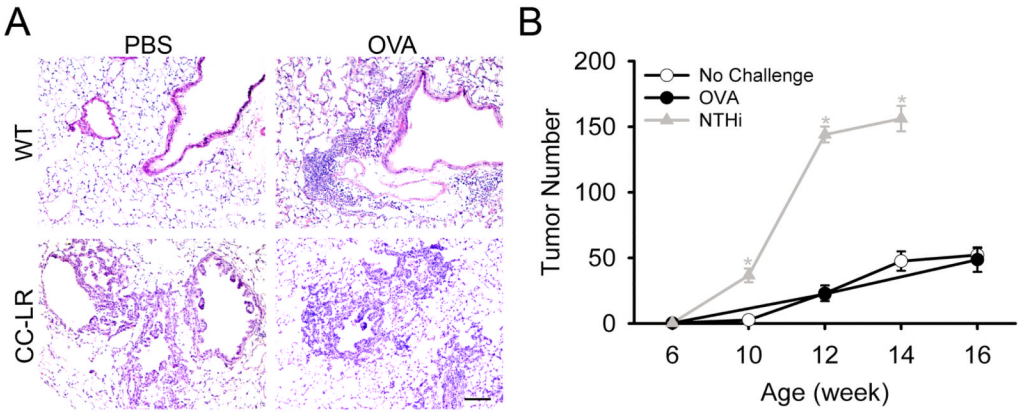

Figure 2. Histopathological analysis of inflammation and tumor progression in lungs after repetitive OVA aerosol exposure

Mice were sensitized weekly for two weeks then exposed to OVA aerosol weekly for eight weeks, then sacrificed one day after the last exposure and their lungs processed for light microscopy with hematoxylin and eosin (H&E) staining to study the inflammation and tumor progression. (A) Top two panels are showing H&E stained sections from the lungs of WT mice with or without repetitive OVA aerosol exposure (10×, scale bar = 100 μm). Bottom two panels are showing H&E stained sections from the lungs of CC-LR mice with or without repetitive OVA aerosol exposure (10×, scale bar = 100 μm). (B) Lung surface tumor numbers in CC-LR mice before OVA aerosol exposure (week 6), after 2 weekly OVA sensitization followed by 4 and 8 weekly exposures to the aerosolized OVA (week 12, and 16, closed circles), or without IP sensitization and aerosol exposure (week 12, and 16, open circles) are shown (gray line with triangle representing NTHi exposed CC-LR mice as the historical control, mean ± SE, * = $p < 0.05$ for NTHi exposed vs unexposed).

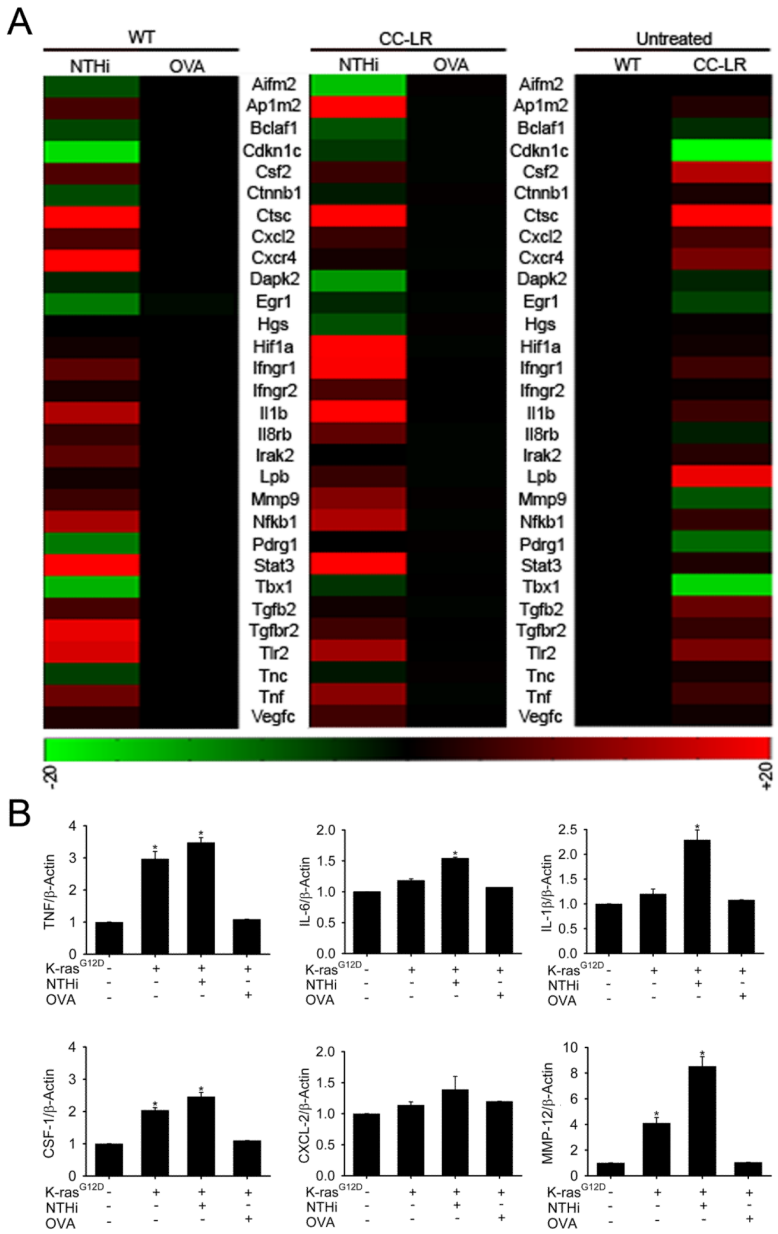

Figure 3. Gene expression analysis of whole lung

(A) Representative of microarray gene expression changes in the whole lung of untreated CC-LR mice compare to untreated WT mice (left panels). Expression changes of the same genes in WT mice (middle panel) and CC-LR mice (right panel) one day after repetitive NTHi lysate treatment compare to the one with repetitive OVA treatment (red, increased gene expression; green, decreased gene expression). (B) Quantitative PCR was done on the RNA extracted from whole lung tissue of WT, CC-LR, and CC-LR mice exposed to NTHi, or OVA and relative mRNA expression of selected genes was calculated and graphed (normalized to β-actin expression level, mean ± SE, * = $P < 0.05$ for CC-LR, or CC-LR with NTHi, or with OVA exposure vs WT).

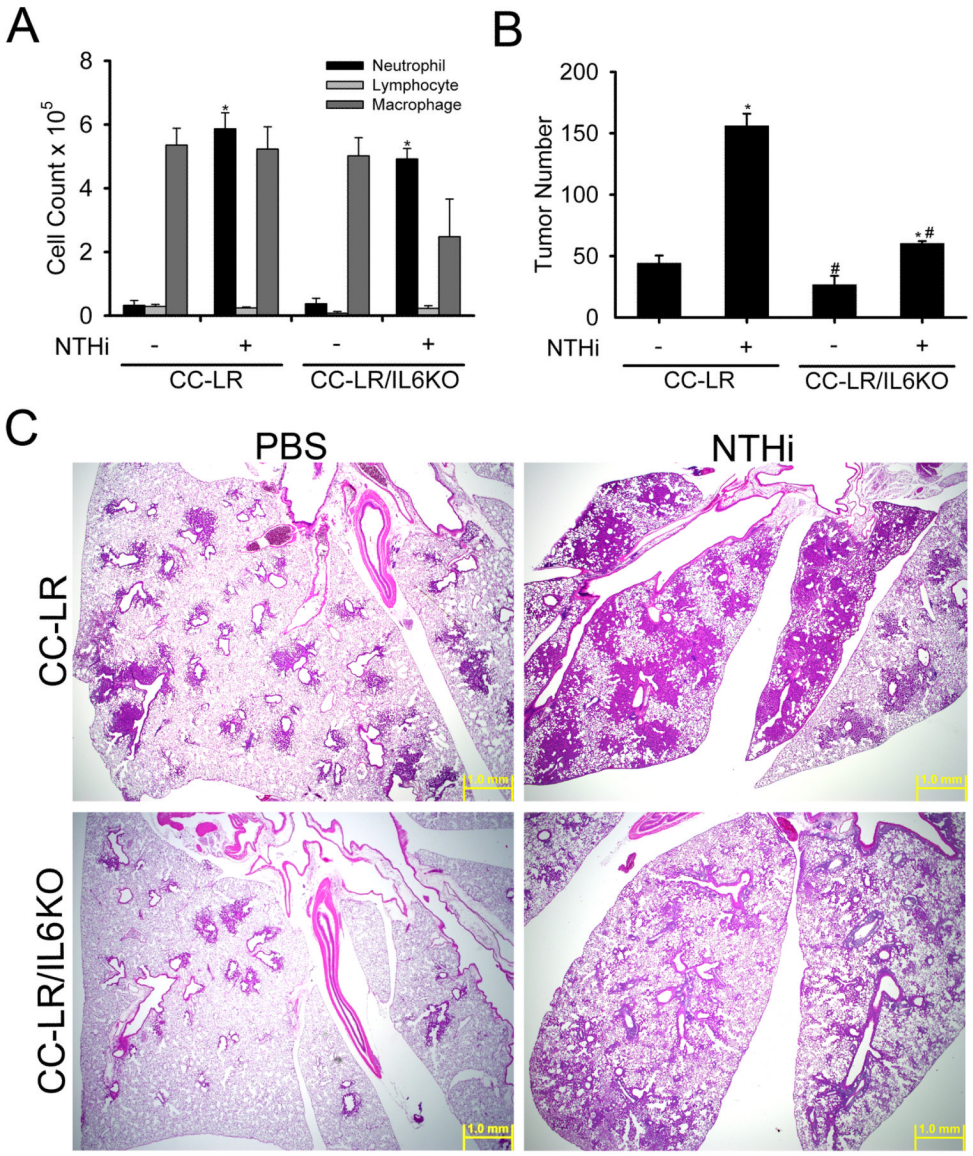

Figure 4. Role of IL-6 in tumor promotion

(A) CC-LR and CC-LR/IL6KO mice were exposed to an NTHi lysate aerosol starting at age 6 weeks weekly for eight weeks. Total and lineage-specific leukocyte numbers in BALF one day after last NTHi aerosol exposure are shown (mean ± SE, * = $p < 0.05$ for CC-LR or CC-LR/IL6KO with NTHi exposure vs without NTHi exposure). (B) Lung surface tumor numbers in CC-LR and CC-LR/IL6KO mice at age 14 weeks with or without 8 weekly NTHi aerosol exposure from age 6 weeks are shown (mean ± SE, * = $p < 0.05$ for CC-LR or CC-LR/IL6KO with NTHi exposure vs without NTHi exposure, # = $p < 0.05$ for CC-LR without NTHi exposure vs CC-LR/IL6KO without NTHi exposure or CC-LR with NTHi exposure vs CC-LR/IL6KO with NTHi exposure). (C) CC-LR and CC-LR/IL6KO mice were exposed weekly for 8 weeks to an NTHi aerosol, and then sacrificed the first day after the last exposure and stained with hematoxylin and eosin (H&E). Top two panels are showing H&E stained sections from the lungs of CC-LR mice with or without repetitive NTHi aerosol exposure (2×, scale bar = 1mm). Bottom two panels are showing H&E stained sections from the lungs of CC-LR/IL6KO mice with or without repetitive OVA aerosol exposure (2×, scale bar = 1mm).

Table 1

Cytokine levels in BALF after OVA exposure

Cytokines	WT			CC-LR		
	- OVA	+ OVA*	FC#	- OVA	+ OVA*	FC#
Inflammatory						
TNF	4.3 ± 0.5	43.8 ± 12.9	10.2	28.1 ± 6.1	34.8 ± 0.6	1.2
IL-1β	4.9 ± 0.7	7.2 ± 0.7	1.4	7.4 ±1.3	5.5 ± 0.6	0.7
IL-6	9.9 ± 1.5	33.3 ± 2.3	3.3	608.4 ±145.7	302.7 ± 79.6	0.5
Th1						
IFN-γ	1.4 ± 0.03	0.9 ± 0.2	0.6	6.0 ± 1.8	2.3 ± 0.7	0.4
Th2						
IL-4	1.4 ± 0.1	34.0 ± 5.4	24.3	1.1 ± 0.3	25.2 ± 1.1	22.9
IL-13	1.8 ± 0.4	6.5 ± 1.3	3.6	2.6 ± 0.4	7.9 ± 0.9	3.1
Th17						
IL-17	0.4 ± 0.2	1.1 ± 0.1	2.7	3.7 ± 0.6	3.5 ± 0.3	0.9
Chemokine						
KC	2.1 ± 0.8	6.1 ± 2.5	2.9	13.7 ± 2.5	34.5 ± 5.5	2.5
Eotaxin	2.9 ± 1.1	15.1 ± 2.4	5.2	2.8 ± 1.1	23.3 ± 7.3	8.3

*BALFs were collected the first day after the 8th OVA exposure. All data are the mean ± SEM, and are expressed as pg/ml.

#Fold change (+OVA/-OVA)

BALF, bronchoalveolar lavage fluid; OVA, ovalbumin; CC-LR, $CCSP^{Cre}$/LSL–K-ras^{G12D}; TNF, tumor necrosis factor; IL-1β, interleukin 1 beta; IL-6, interleukin 6; IFN-γ, interferon gamma; IL-4, interleukin 4; IL-13, interleukin 13; IL-17, interleukin 17; KC, keratinocyte-derived chemokine.

Table 2

Comparison of gene expression changes presented as fold changes

Symbol	Category and Definition	CC-LR/WT	WT+NTHi/WT	CC-LR+NTHi/CC-LR	WT+OVA/WT	CC-LR+OVA/CC-LR	Accession Number
	INFLAMMATORY						
Il1b	interleukin 1 beta	146.80	218.5	4.9	59.1	0.90	NM_008361
Il6	interleukin 6	17.00	14.6	1.6	-5.9	-3.90	NM_031168.1
Il12b	interleukin 12 beta	87.00	12.7	-9.0	-12.5	-50.30	NM_008352.2
Il17f	interleukin 17f	7.40	17.6	1.1	-0.02	-10.50	NM_145856.1
Il18	inteleukin 18	2.60	1.6	3.6	0.2	1.20	NM_008360.1
TNF	tumor necrosis factor	17.50	51.2	3.1	-19	-7.20	NM_144548.1
Il17ra	interleukin 17 receptor A	1.10	1.7	3.3	0.7	0.05	NM_013693.1
Il8rb	interluekin 8 recepto, beta	27.20	24	4.5	0.8	-2.20	NM_008359.1
Cxcl2	chemokine (C-C motif) receptor 2	39.90	33.6	2.5	-0.9	-0.60	NM_009909.3
Cxcr4	chemokine (C-X-C motif) receptor 4	238.80	157.5	1.4	19.7	-0.06	NM_009915.1
Cxcl4	chemokine (C-X-C motif) ligand 4	1.60	0.7	2.9	1.3	0.46	NM_009140.2
Ifngr1	interferon gamma receptor 1	2.20	2.7	1.8	0.9	1.10	NM_009911.2
Ifngr2	interferon gamma receptor 2	1.30	4.1	1.6	1.5	0.80	NM_019932.2
Ifi30	interferon gamma inducible protein 30	2.60	3.5	2.2	1.3	1.03	NM_010511.2
	IMMUNE RESPONSE						
Nfkb1	nuclear factor of kappa light polypeptide gene enhancer in B-cells, 1 p105	1.60	2.4	1.4	1.2	0.51	NM_008689.2
Nfkb2	nuclear factor of kapp light polypeptide gene enhancer in B cells 2	79.70	40.9	1.5	31.5	0.07	NM_019408.1
Stat3	signal transducer and activator of transcription 3	2.50	3.5	1.9	0.7	0.30	NM_011486.4
Ap1m2	adaptor protein complex AP-1, mu 2 subunit	6.80	44.8	1.8	0.3	0.40	NM_009678.1
Tlr2	toll-like receptor 2	381.50	250.7	3.3	4.4	0.80	NM_011905.2
Tlr4	toll-like receptor 4	13.60	14.4	1.5	-0.7	0.60	NM_021297.2
Tlr6	toll-like receptor 6	81.70	45.6	1.2	-1.8	0.26	NM_011604.2
Tlr7	toll-like receptor 7	21.30	7.1	1.8	5.7	0.89	NM_133211.3
Irak2	interleukin-1 receptor-associated kinase 2	2.40	1.9	1.7	0.7	0.37	NM_172161.2
Raet1a	retinoic acid early transcript 1, alpha	9.10	12.1	0.1	-5.2	-3.70	NM_009016.1
S100a8	S100 calcium binding protein A8	2.20	2.1	2.1	1.6	0.80	NM_013650.2

Symbol	Category and Definition	CC-LR/WT	WT+NTHi/WT	CC-LR+NTHi/CC-LR	WT+OVA/WT	CC-LR+OVA/CC-LR	Accession Number
Kng1	kininogen 1	3.60	17.2	2.2	2.3	1.70	NM_023125.2
Kng2	kininogen 2	8.50	2.2	5.6	0.8	0.70	NM_201375.1
Lbp	lipopolysaccharide binding protein	3.30	1.3	1.3	0.4	0.50	NM_008489.2
Cd68	CD68 antigen	54.90	7.1	1.4	6.3	1.10	NM_009853.1
	CELL CYCLE AND GROWTH						
Fgf7	fibroblast growth factor 7	2.60	2.6	1.2	0.5	-1.60	NM_008008.3
Myc	myelocytomatosis oncogene	12.00	5.5	1.3	-5	3.30	NM_010849.4
Ereg	epiregulin	5.70	5.9	2.3	-6.9	-4.80	NM_007950.1
Cdkn2a	cyclin-dependent kinase inhibitor 2A	17.90	18.9	1.1	-3.3	-2.60	NM_009877.2
Fgfr2	fibroblast growth factor receptor 2	20.00	16.4	5.5	0.7	2.20	NM_010207.2
Itm2b	integral membrane protein 2B	1.90	1.8	1.2	-1.75	0.51	NM_008410.2
Csf1r	colony stimulating factor 1 receptor	13.90	16.1	2.3	1.7	2.60	NM_001037859.2
Csf2	colony stimulating factor 2	244.50	41.6	2.0	7.5	0.40	NM_009969.4
Csf2ra	colony stimulating factor 2 receptor, alpha	354.40	150.3	1.2	40.3	0.20	NM_009970.1
Socs3	suppressor of cytokine signaling 3	2.70	1.6	1.1	1.4	0.90	NM_007707.2
Cdkn1a	cyclin-dependent kinase inhibitor 1A	5.90	3.4	1.7	4.1	1.10	NM_007669.2
Emr1	EGF-like module containing, mucin-like, hormone receptor-like sequence 1	14.70	75.2	2.1	19.2	1.10	NM_010130.1
Areg	amphiregulin	9.90	1.6	1.2	1.1	0.80	NM_009704.3
	CELL DEATH AND APOPTOSIS						
Cideb	cell death-inducing DNA fragmentation factor, alpha subunit-like effector B	67.40	21.5	1.4	-2.7	0.60	NM_009894.2
Bcl2l14	Bcl2-like protein14	29.70	30.2	1.5	-25.6	-4.00	NM_025778.1
Bcl2a1c	B-cell leukemia/lymphoma 2 related protein A1c	233.00	42.6	2.5	-0.1	0.07	NM_007535.2
	ANGIOGENESIS, INVASION AND METASTASIS						
Pdgfc	platelet-derived growth factor, C polypeptide	29.40	18.3	1.8	9.4	1.20	NM_019971.2
Vegfc	vascular endothelial growth factor C	2.30	2.7	1.4	2.1	1.60	NM_009506.2
Hbegf	heparin-binding EGF-like growth factor	1.10	1.1	1.5	1.6	2.10	NM_010415.1
Hif1a	hypoxia inducible factor 1, alpha subunit	23.60	17.4	6.6	-41.7	-6.50	NM_010431.1
Icam1	intercellular adhesion molecule 1	6.80	4.5	3.4	2.1	0.80	NM_010493.2
Pecam1	platelet/endothelial cell adhesion molecule 1	1.90	3.1	1.9	0.6	0.50	NM_008816.2

Symbol	Category and Definition	CC-LR/WT	WT+NTHi/WT	CC-LR+NTHi/CC-LR	WT+OVA/WT	CC-LR+OVA/CC-LR	Accession Number
Mmp2	matrix metallopeptidase 2	1.40	3.3	1.2	0.3	0.30	NM_008610.2
Mmp12	matrix metallopeptidase 12	2827.00	305.5	5.0	299.4	0.40	NM_008605.3
Mmp14	matrix metallopeptidase 14	1.90	2.9	1.3	1.9	0.40	NM_008608.2
Timp1	tissue inhibitor of metalloproteinase 1	9.30	17.4	1.4	2.4	1.20	NM_011593
Nus1	nuclear undecaprenyl pyrophosphate synthase 1 homolog	301.20	72.5	1.4	11.6	0.40	NM_030250.1
Ang	angiogenin	2.50	1.9	1.5	0.8	0.70	NM_007447.2
Tgfbr1	transforming growth factor, beta receptor I	3.40	4.9	1.5	0.9	0.70	NM_009370.2
Tgfbr2	transforming growth factor, beta receptor II	2.40	2.2	2.2	0.5	0.90	NM_009371.2
Lcn2	lipocalin 2	9.70	15.4	2.1	7.2	0.80	NM_008491.1
	PROTEIN SYNTHESIS, TURNOVER AND TARGETING						
Eif1a	eukaryotic translation initiation factor 1A	1.90	1.3	1.1	0.7	0.62	NM_025437.4
Kras	v-Ki-ras2 Kirsten rat sarcoma viral oncogene homolog	2.30	0.3	1.1	0.5	0.70	NM_021284.4
Hras1	Harvey rat sarcoma virus oncogene 1	1.80	1.9	1.2	1.8	-0.08	NM_008284.1
Nola2	nucleolar protein family A, member 2	2.10	1.8	1.8	0.8	0.50	NM_026631.3
Nol5A	nucleolar protein 5A	56.70	7.6	2.3	-1.8	-0.57	NM_024193.2
Nup62	nucleoporin 62	2.90	1.5	1.1	1.1	0.72	NM_053074.1
Rasl11a	RAS-like, family 11, member A	5.30	2.4	1.9	3	0.58	NM_026864.1
Rhog	ras homolog gene family, member G	1.50	0.9	1.3	1.6	1.36	NM_019566.3
Ctsc	cathepsin C	9.10	7.8	1.7	2.9	0.87	NM_009982.2
Sdcbp2	syndecan binding protein	2.40	9.3	16.8	0.2	-0.48	NM_001098227.1
	MORPHOGENESIS						
Krt19	keratin 19	26.30	18.1	1.2	15.7	0.55	NM_008471.2
Krt23	keratin 23	3.60	1.3	1.3	0.7	0.70	NM_033373.1
Lamc2	laminin, gamma 2	30.10	67.2	1.9	-13.7	-0.50	NM_008485.3
Sftpb	surfactant associated protein B	3.40	1.3	1.5	0.9	0.40	NM_147779.1
	TRANSCRIPTION AND CHROMATIN STRUCTURE						
Bhlhb8	basic helix-loop-helix domain containing, class B, 8	2.10	1.4	1.7	1.1	2.10	NM_010800.3
Ddx39	DEAD (Asp-Glu-Ala-Asp) box polypeptide 39	19.90	16.5	1.1	5.8	0.66	NM_197982.2
Lmna	lamin A	9.10	5.8	1.1	2	0.80	NM_019390.1

Symbol	Category and Definition	CC-LR/WT	WT+NTHi/WT	CC-LR+NTHi/CC-LR	WT+OVA/WT	CC-LR+OVA/CC-LR	Accession Number
Pparg	peroxisome proliferator activated receptor gamma	18.60	12.7	2.8	1.1	1.60	NM_011146.2
Spib	Spi-B transcription factor (Spi-1/PU.1 related)	18.40	35.9	1.0	13	-4.80	NM_019866.1